

Supporting Information

for

**Comparative Study of H₂ Sensing Performance of Stoichiometric
Polymorphs of Titanium Carbide MXenes Loaded with Pd NDs**

Zhiwei Yang¹, Lijuan Dong¹, Qian Chen², Zeyi Wang¹, Jiacheng Cao², Mengwei
Dong¹, Jian Wang¹, Jian Zhang^{1*}, Xiao Huang^{1*}

1. Institute of Advanced Materials (IAM), Nanjing Tech University (NanjingTech),
30 South Puzhu Road, Nanjing 211816, P.R. China;

2. Frontiers Science Center for Flexible Electronics, Xi'an Institute of Flexible
Electronics (IFE) and Xi'an Institute of Biomedical Materials & Engineering,
Northwestern Polytechnical University, 127 West Youyi Road, Xi'an 710072, China.

* Corresponding authors: Jian Zhang, Xiao Huang

E-mail addresses: iamjzhang@njtech.edu.cn, iamxhuang@njtech.edu.cn

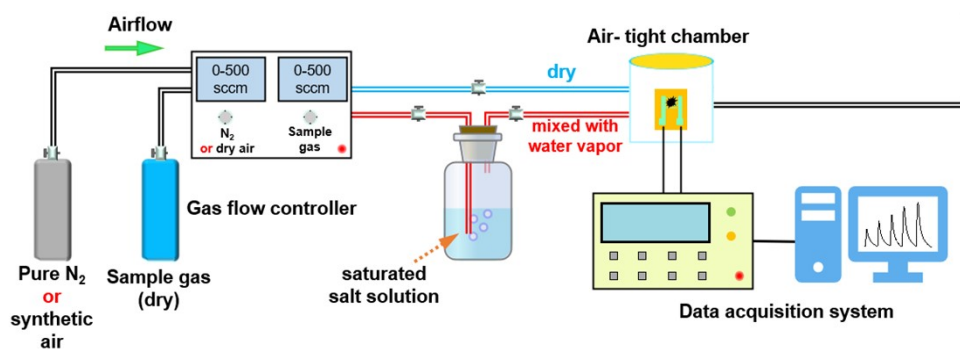


Fig. S1 Schematic of the gas sensing setup used in this study. The target gases with specific concentrations were obtained by changing the flow rates of the sample gas and the carrier gas, i.e. N_2 or dry air. As for humid air sensing, the relative humidity (RH) was controlled by passing the target gas through a bottle of saturated salt solution. The type of saturated solutions (LiF , $MgCl$ and $NaNO_3$ for 11%, 33% and 74% RH, respectively) determines the relative humidity.

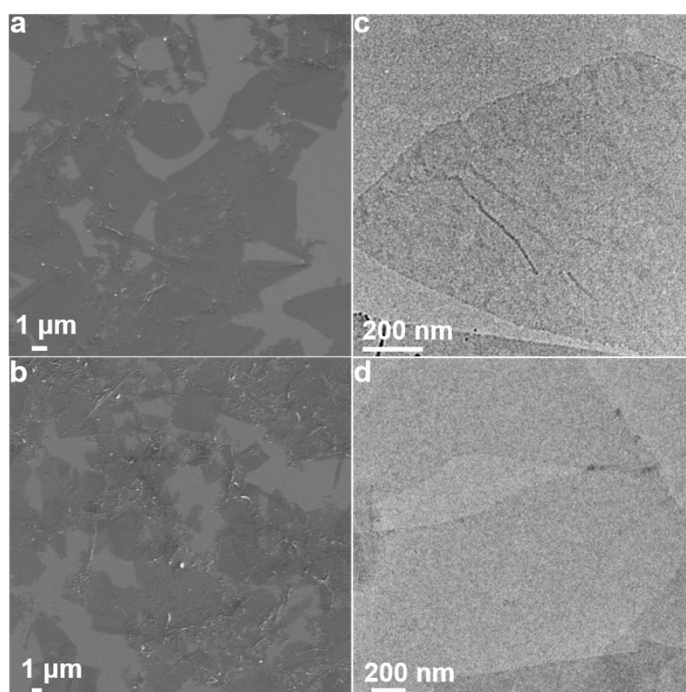


Fig. S2 SEM images of (a) Ti_2CT_x and (b) $Ti_3C_2T_x$; TEM images of (c) Ti_2CT_x and (d) $Ti_3C_2T_x$.

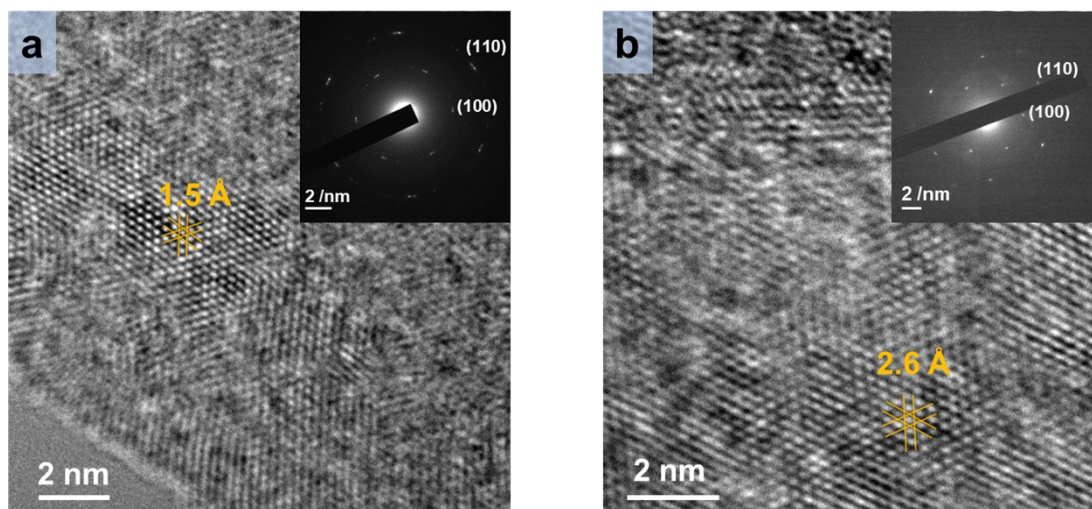


Fig. S3 High-magnification TEM images of (a) Ti_2CT_x and (b) $\text{Ti}_3\text{C}_2\text{T}_x$; insets show the corresponding electron diffraction pattern.

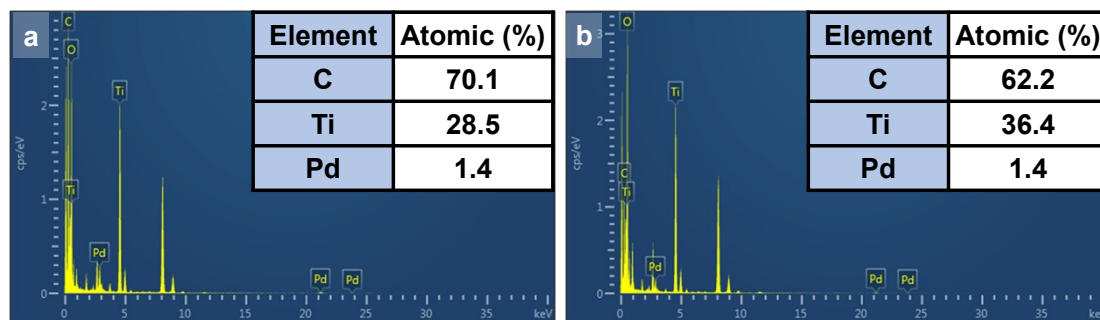


Fig. S4 Atomic ratio of elements based on EDX mapping results. (a) $\text{Pd}/\text{Ti}_2\text{CT}_x$; (b) $\text{Pd}/\text{Ti}_3\text{C}_2\text{T}_x$.

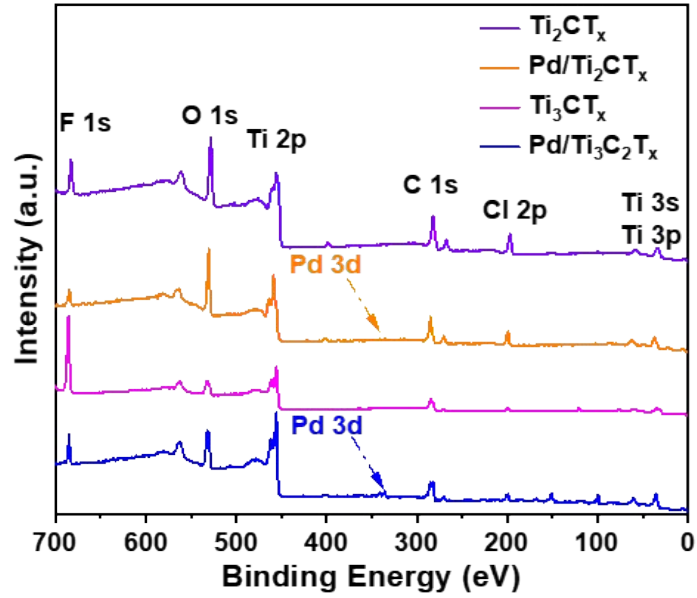


Fig. S5 XPS full spectra of as-prepared samples.

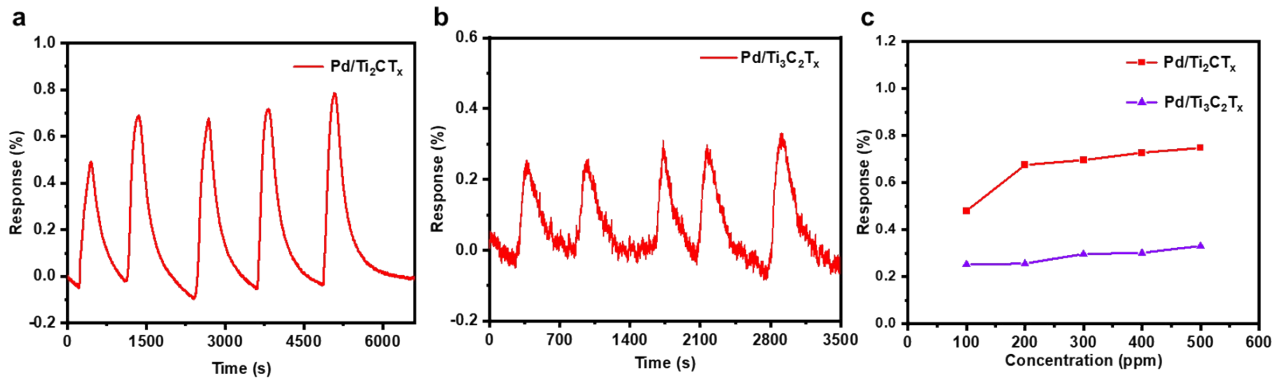


Fig. S6 Gas sensing performance of Pd/MXene in dry air. Dynamic response-recovery curves of (a) Pd/Ti₂CT_x and (b) Pd/Ti₃C₂T_x to different concentration of H₂ after baseline removal. (c) Relationships between H₂ concentration and responses of Pd/Ti₂CT_x and Pd/Ti₃C₂T_x.

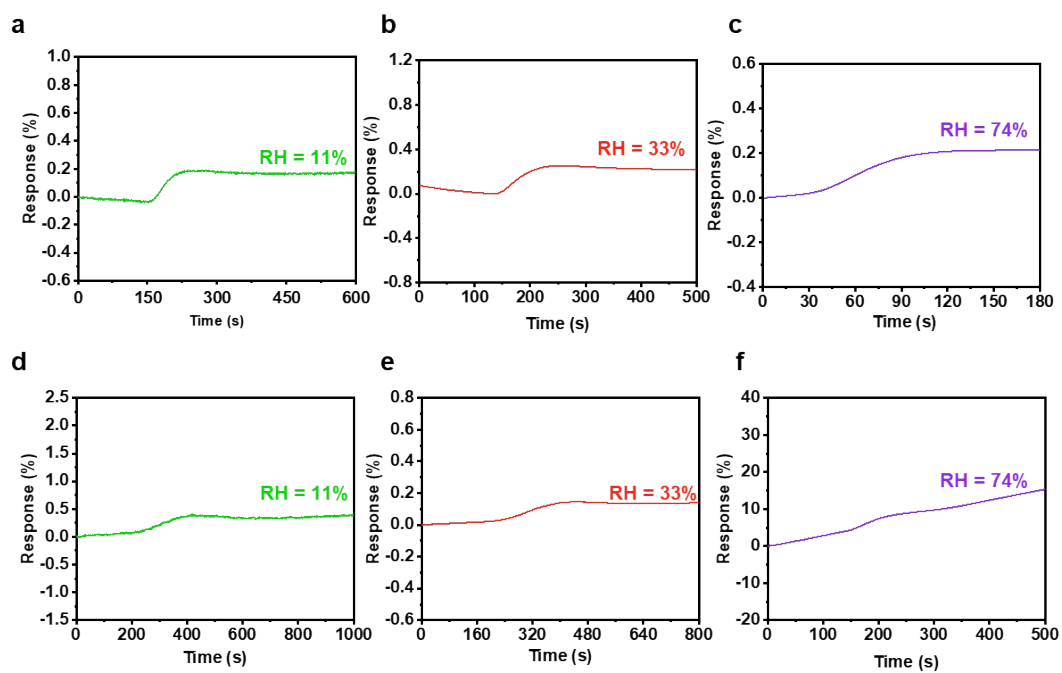


Fig. S7 Gas sensing performance of Pd/MXene in humid air. Response of (a-c) Pd/Ti₂CT_x and (d-f) Pd/Ti₃C₂T_x nanosheets upon exposure to 200 ppm of H₂ with different humidity.

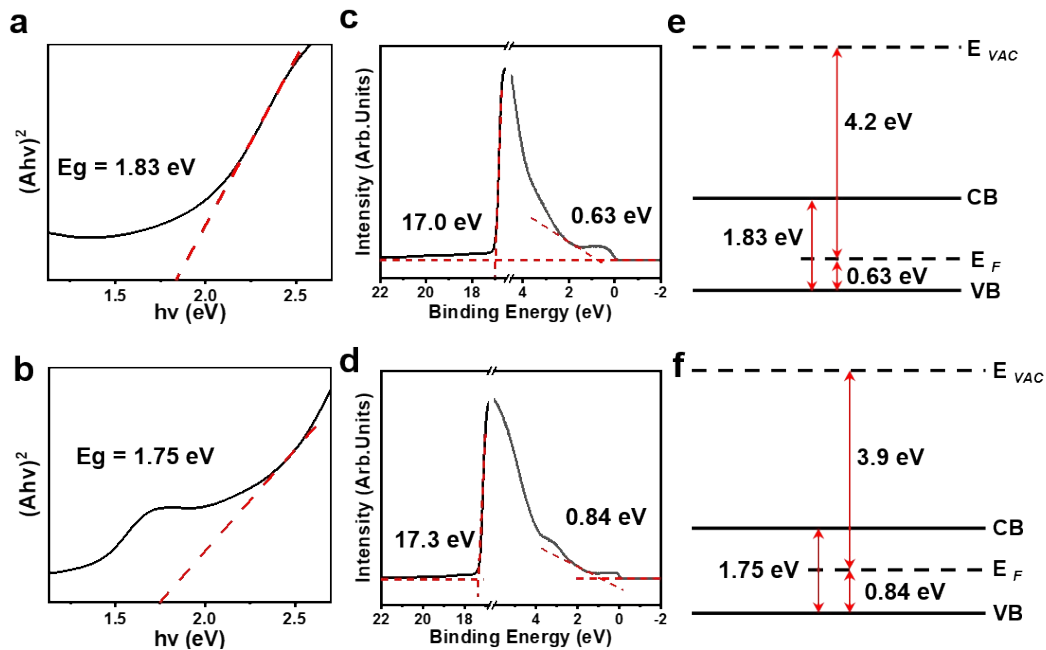


Fig. S8 Optical absorption spectra of (a) Ti_2CT_x and (b) $\text{Ti}_3\text{C}_2\text{T}_x$, showing the plots of $(\alpha h\nu)^2$ against photon energy. UPS and XPS valence spectra of (c) Ti_2CT_x and (d) $\text{Ti}_3\text{C}_2\text{T}_x$. The corresponding energy band structures of (e) Ti_2CT_x and (f) $\text{Ti}_3\text{C}_2\text{T}_x$ based on the UV-vis, UPS and XPS results.

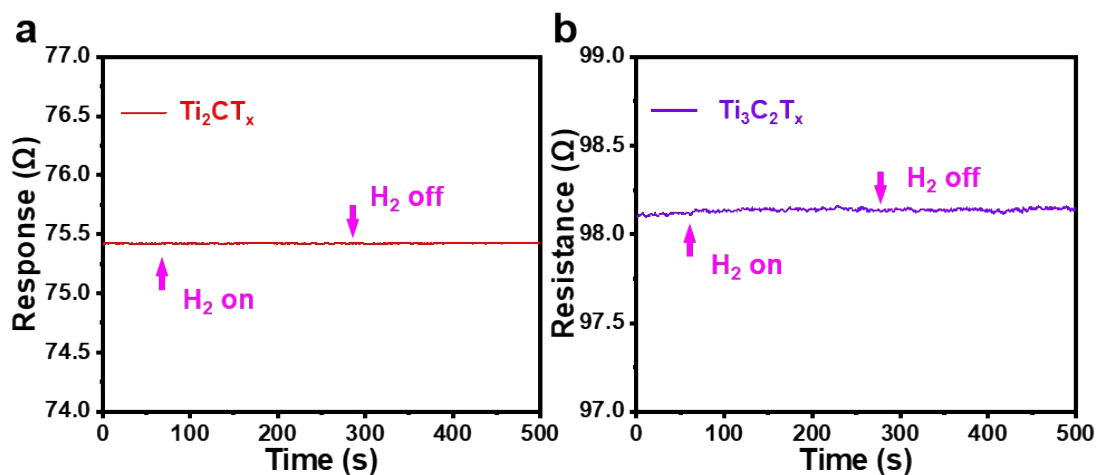


Fig. S9 Dynamic response-recovery curves of the bare Ti_2CT_x (a) and the bare $\text{Ti}_3\text{C}_2\text{T}_x$ (b) to 200 ppm H_2 at room temperature.

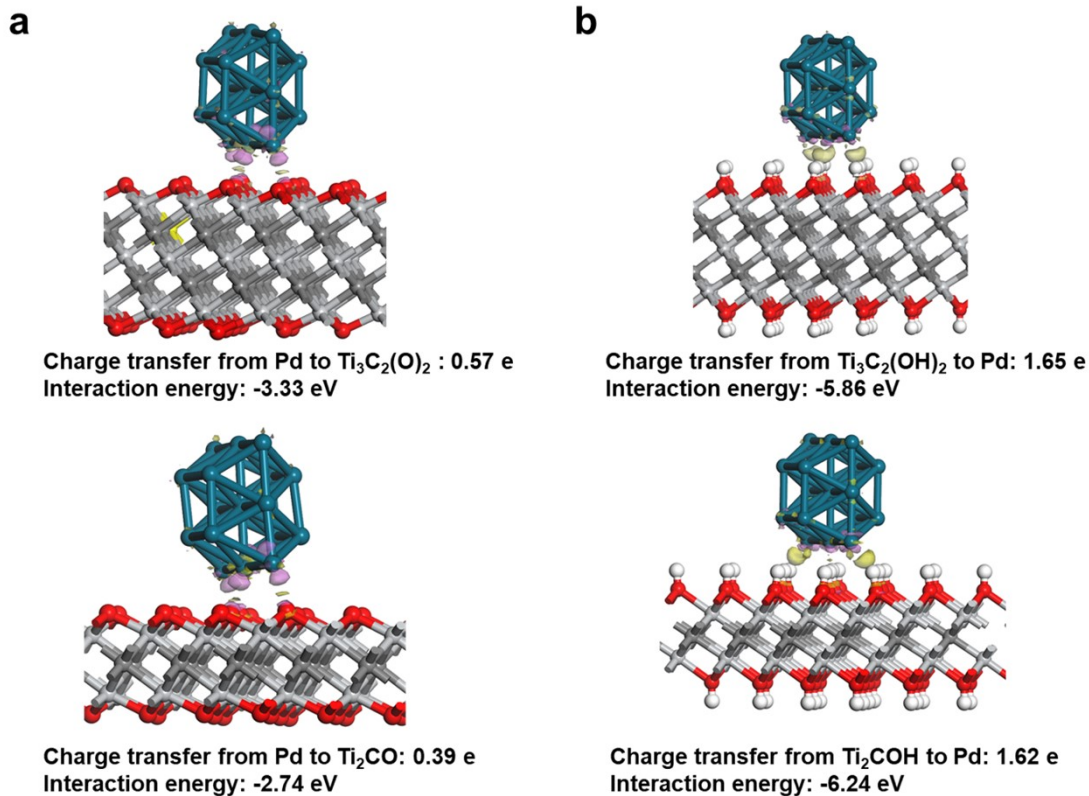


Fig. S10 Simulated electron density difference distribution of Pd/ Ti_2C and Pd/ Ti_3C_2 with epoxy functional groups (a) and hydroxyl function groups (b). Yellow indicates electron deficient regions and purple indicates electron rich regions.

The calculated results indicate that MXenes with epoxy function groups act as charge acceptors, and the charge transfer from Pd to $\text{Ti}_3\text{C}_2(\text{O})_2$ (0.57 e) is higher than that of Ti_2CO (0.39 e). While MXenes with hydroxyl function groups act as charge donors, and the charge transfer from $\text{Ti}_3\text{C}_2(\text{OH})_2$ to Pd (1.65) is similar to that of Ti_2COH (1.62 e). To further detail the charge transfer differences between MXenes and Pd nanodots, the ratio of epoxy function groups to hydroxyl function groups was firstly calculated by extracting the XPS fitting peak area. Afterwards, based on the ratio of function groups, the charge transfer from Ti_2CT_x to Pd was calculated as 1.34 e, which is higher than that of $\text{Ti}_3\text{C}_2\text{T}_x$ (1.2), in accordance with the results that obtained from theoretical model without functional groups.